REFERENCES

1. J. Kennedy and R. Eberhart, Particle swarm optimization, In International Conference on Neural Networks (ICNN'95), Perth, WA, 1995, pp. 1942–1948.
2. D. Karaboga, An idea based on honey bee swarm for numerical optimization, Tech Report-TR06, Eng Fac Comput Eng Dep ERCIYES Univ, 2005.
3. M. Dorigo, Optimization, learning and natural algorithms, Politecnico di Milano, Milano, Italy, 1992.
4. M.C. Alcantara Neto, J.P.L. Araújo, F.J.B. Barros, A.N. Silva, G.P.S. Cavalcante, and A.G. D'Assunção, Bioinspired multiobjective synthesis of X-band FSS via general regression neural network and cuckoo search algorithm, Microw Opt Technol Lett 57 (2015), 2400–2405.
5. E. Bonabeau, G. Theraulaz, and M. Dorigo, Swarm intelligence: From natural to artificial systems, Oxford University Press, New York, 1999.
6. J. Robinson and Y. Rahmat-Samii, Particle swarm optimization in electromagnetics, IEEE Trans Antennas Propag 52 (2004), 397–407.
7. Y.L. Li, W. Shao, L. You, and B.Z. Wang, An improved PSO algorithm and its application to UWB antenna design, IEEE Antennas Wirel Propag Lett 12 (2013), 1236–1239.
8. P.H.F. Silva, R.M.S. Cruz, and A.G. D'Aassunção, Blending PSO and ANN for optimal design of FSS filters with koch Island patch elements, IEEE Trans Magn 46 (2010), 3010–3013.
9. S. Grubisic, W.P. Carpes, Jr., J.P.A. Bastos, and G. Santos, Association of a PSO optimizer with a quasi-3D ray-tracing propagation model for mono and multi-criterion antenna positioning in indoor environments, IEEE Trans Magn 49 (2013), 1645–1648.
10. R.A. Vural, S. Member, and T. Yildirim, Performance evaluation of evolutionary algorithms for optimal filter design, IEEE Trans Evol Comput 16 (2012), 135–147.
11. T.K.K. Tsang and M. N. El-Gamal, Ultra-wideband (UWB) communications systems: An overview, In The 3rd IEEE-NEWCAS International Conference, Québec, Canada, 2005, pp. 381–386.
12. A. M. Ben, Frequency selective surfaces: Theory and design, Wiley, Hoboken, NJ, USA, 2005.
13. E. Cuevas, M. Cienfuegos, D. Zaldívar, and M. Pérez-Cisneros, A swarm optimization algorithm inspired in the behavior of the social-spider, Expert Syst Appl 40 (2013), 6374–6384.
14. W.C. Araújo, H.W.C. Lins, A.G. D'Assunção, Jr., J.L.G. Medeiros, and A.G. D'Assunção, A bioinspired hybrid optimization algorithm for designing broadband frequency selective surfaces, Microw Opt Technol Lett 56 (2014), 329–333.
15. M.R. da Silva, C.L. Nóbrega, P.H.F. Silva, and A.G. D'Assunção, Optimization of FSS with Sierpinski island fractal elements using population-based search algorithms and MLP neural network, Microw Opt Technol Lett 56 (2014), 827–831.
16. A. Anuradha, A. Patnaik, and S.N. Sinha, Design of custom-made fractal multi-band antennas using ANN-PSO, IEEE Antennas Propag Mag 53 (2011), 94–101.
17. C.R.M. Silva, H.W.C. Lins, S.R. Martins, E.L.F. Barreto, and A.G. D'Assunção, A multiobjective optimization of a UWB antenna using a self organizing genetic algorithm, Microwave Opt Technol Lett 54 (2012), 1824–1828.
18. P.H.F. Silva, C.L. Nóbrega, M.R. Silva, and A.G. D'Assunção, Optimal design of frequency selective surfaces with fractal motifs, IET Microwaves Antennas Propag 8 (2014), 627–631.

COMPACT MILLIMETER-WAVE SWITCHED-BEAM ANTENNA ARRAYS FOR SHORT RANGE COMMUNICATIONS

A. T. Alreshaid,[1] M. S. Sharawi,[1] S. Podilchak,[2] and K. Sarabandi[3]

[1] Electrical Engineering Department, King Fahd University of Petroleum & Minerals, Dhahran, 31261, Saudia Arabia; Corresponding author: msharawi@kfupm.edu.sa

[2] Institute of Sensors, Signals and Systems within the School of Engineering and Physical Sciences at Heriot-Watt University, Edinburgh, Scotland EH14 4AS, United Kingdom

[3] Electrical and Computer Engineering Department, University of Michigan, Ann arbor, MI 48109

Received 16 December 2015

ABSTRACT: *The need for more data throughput is a requirement that will keep growing in future wireless standards, and during the past few years, millimeter-wave technology has generated much excitement in the mobile and wireless communications sectors due to the large bandwidth it can offer. In this letter two different travelling-wave, slot antenna arrays are proposed which can offer tunable switched-beam capability at millimeter-wave frequencies. The antenna systems are built on a single layer PCB with top- and bottom-side etching for operation at 28 GHz with at least 0.7 GHz of measured impedance bandwidth. For the first design, a planar 2 × 4 slot antenna array is proposed while the second design is implemented using a 4 × 4 slot array to demonstrate improved beam directivity. A Butler matrix for simple beam switching in the far-field is also integrated within the compact antenna structure to provide the needed phased array operation. The total size of the two proposed systems with their feed networks are 55.2 × 55 × 0.13 mm^3 and 53.7 × 61.2 × 0.13 mm^3, respectively. These new travelling-wave switched beam arrays can be placed within current handheld mobile devices for high bandwidth short range communications enabling 5G technologies.* © 2016 Wiley Periodicals, Inc. Microwave Opt Technol Lett 58:1917–1921, 2016; View this article online at wileyonlinelibrary.com. DOI 10.1002/mop.29940

Key words: *Butler beam-forming network; millimeter-wave; slot antenna; switched beam; traveling-wave antenna; 5G*

1. INTRODUCTION

The exponential increase in the volume of data traffic has motivated researchers to start exploring and nominating the millimeter-wave (mm-wave) spectrum as a candidate to provide channels with large bandwidths (BWs) for fifth generation (5G) wireless communication systems. All wireless standards operating in the frequency range from 700 MHz to 2.6 GHz have limited channel BWs, thus limiting the amount of data for transmission. By up converting the communication frequency to 28 GHz or 38 GHz the allocated BW can increase significantly, providing data speeds much higher than what is provided by the latest technology launched to-date, more specifically, long-term-evolution advanced (LTE-A).

This immediate need for high data throughput at millimeter-wave frequencies can be met by utilizing robust radio access technologies. However, when considering frequency systems operating around 60 GHz, for example, high path loss due to atmospheric absorption can be observed. On the other hand, it was recently found that the attenuation caused by this phenomena at 28 GHz is only 0.012 dB over 200 m and 0.016 dB over the same distance at 38 GHz, thus providing a good frequency candidate for future wireless systems and enabling the possibility for high data rate throughputs with large BWs [1,2]. Moreover, by taking advantage of the 28 GHz operational frequency, the corresponding wavelength is much smaller than more conventional communication schemes and thus mobile devices can support more antenna elements and arrays for higher gain. This can compensate for the free-space path losses introduced in the millimeter-wave communications channel.

The design of such 5G mobile terminals employing compact and tunable traveling-wave arrays with switched-beam capability, and other leaky-wave phased arrays [3] for wireless

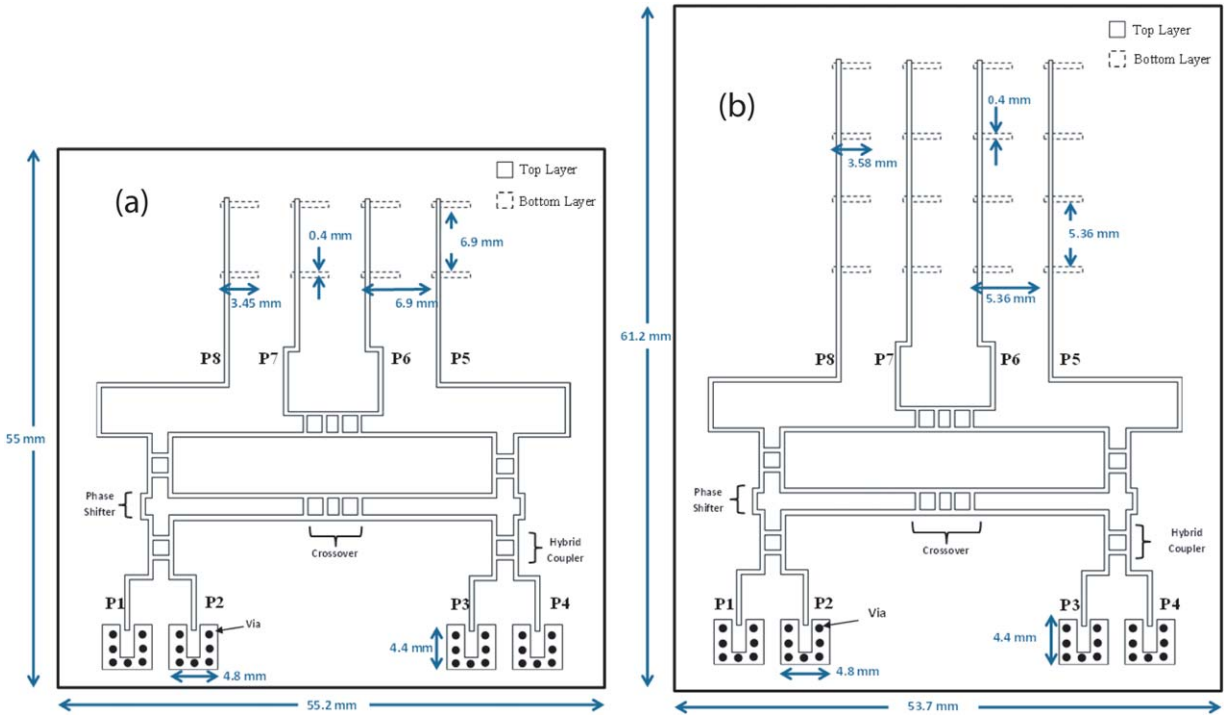

Figure 1 Layouts of Butler network integrated with a (a) 2 × 4 and a (b) 4 × 4 slot antenna array. [Color figure can be viewed in the online issue, which is available at wileyonlinelibrary.com]

technologies at millimeter-wave frequencies, has not been widely investigated in the literature. There have been a few notable works at microwave frequencies where tunable series-fed patch antenna array elements, using new phased array approaches, have been demonstrated [4–6]. However, additional antenna research should be encouraged to meet the needs for beam controllable millimeter-wave antenna arrays enabling the aforementioned short-range communications. This is because with a limited number of radiating elements, compact series-fed antenna arrays can offer beam directivities on the order of 10 dB with half-power beam widths which are typically less than 8°.

To enable pattern control for these types of traveling-wave antennas using simpler phased array approaches, beam-forming networks are needed for pattern switching and control in the far-field. The Butler network may be preferred for mobile communications since it is a relatively simple feeding structure with low-losses offering low-cost implementation and simple integration with hand-held terminals. Moreover, few works have concentrated on designing Butler networks at millimeter-wave frequency, such as in Refs. 7,8 at 60 GHz, while the rest of the papers operated below 13 GHz such as in Refs. 9,10. In Ref. 11, for example, a 24 GHz Butler network was designed on silicon using 0.18 μm CMOS technology with no antenna elements for radiation. It provided a BW of 2 GHz where the core Butler circuitry was only 0.9 mm by 0.46 mm, excluding the outer connections and the input/output ports. An integrated Butler with patches was designed in Ref. 11. The operating frequency was 60 GHz providing a BW of 3 GHz. The system was built on an RT/duroid 5880 substrate with dielectric constant of 2.2 and thickness of 0.127 mm. The gain of the antennas was between 7 and 8.9 dBi. Most of the antennas for these systems were based on patches or quasi-yagi antennas in a linear array setup.

In this work, we propose two versions of one of the first traveling-wave antenna arrays using a Butler matrix for switched-beam diversity at 28 GHz. The proposed designs (see Fig. 1) are implemented using an array of series-fed slots printed on a single layer PCB with top- and bottom-side etching. To our knowledge this is the first time that such traveling-wave phased arrays with an integrated beam forming network have been designed, measured, and experimentally verified, while also, offering simple low cost implementation. The first version of the system contains a 2 × 4 slot antenna array integrated with its Butler feed network, while the second version is a similar 4 × 4 array. The measured −10 dB impedance BWs were at least 0.8 GHz and 0.7 GHz for the 2 × 4 and the 4 × 4 array, respectively. In addition, measured gain values for the two designs ranged from 5 to 7 dB and simulations and measurements are presented demonstrating good performance for the compact switched-beam travelling-wave antennas.

2. DESIGN DETAILS

There are several configurations of networks that can provide multi/switched beam control, such as the Butler matrix, the phased array network, and the Rotman and Bootlace lenses [12].

TABLE 1 Antenna Array Design Parameters for the Two Versions

	Slot's Width (mm)	Slot's Length (mm)	Horizontal Shift From Feed's Center (mm)	Inter-Element Spacing (mm)	No. Elements Per Feed (Series)
Version I	0.4	3.45	1.3	6.9	2
Version II	0.4	3.58	1.36	5.36	4

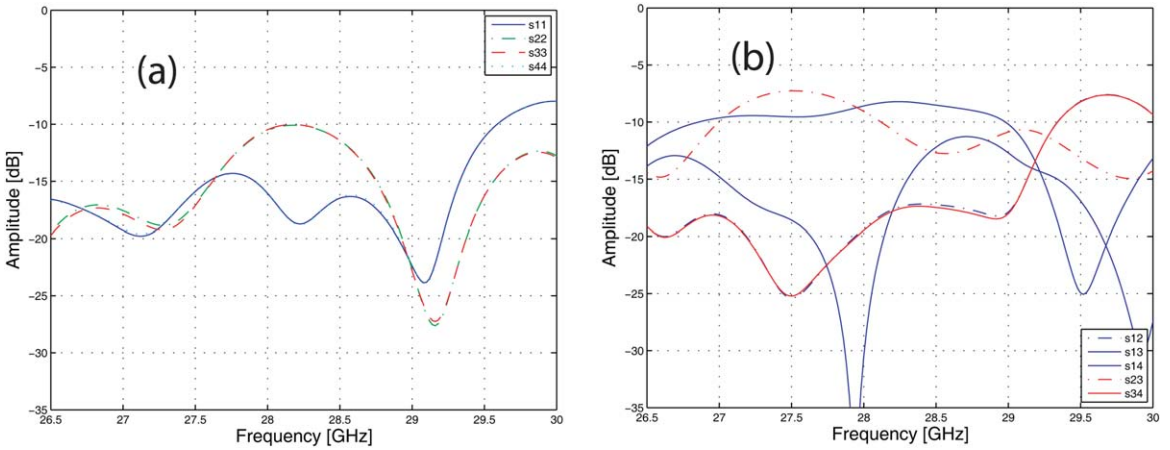

Figure 2 Simulated port parameter curves for the 4 × 4 antenna array, (a) reflection coefficients, (b) port coupling. [Color figure can be viewed in the online issue, which is available at wileyonlinelibrary.com]

They can be classified into different categories; active and passive, steering and non-steering, simple and complex. Each configuration has its own advantages and disadvantages. Due to the Butler network's advantages over other types like its compact design, passive architecture, and the absence of external control, it has been selected to feed the proposed traveling-wave antenna arrays, mainly, to offer low cost, switched beam capability, and simple integration with other electronic components.

In this letter, the Butler beam forming network is 4 × 4, so the insertion phases feeding the traveling-wave arrays are −135°, −45°, +45°, and +135° respectively. This can offer beam steering at broadside for the angles −45°, −20°, +20°, and +45° in a transverse plane perpendicular to the system board. More specifically, our 4 × 4 Butler network for millimeter-wave frequencies consists of 4 couplers, 2 crossovers, and 4 phase delay lines. These feed systems and antenna arrays are built on a thin (0.13 mm) Rogers 3003 substrate with a dielectric constant of 3 to reduce surface wave excitation and improve radiation efficiency. According to these parameters, the width of the microstrip line is 0.33 mm to provide an impedance of 50 Ω. Also, the dimensions of the hybrid coupler arms are 0.19 mm by 2.44 mm for the thin arm (50 Ω) and 0.41mm by 2.2 mm for the thicker one (35.35 Ω). The crossover is achieved by cascading two of these hybrid couplers, which results in passing the two signals across each transmission line with the some loss and phase shift. Figure 1 illustrates the layout of the two proposed antenna arrays while dimensions for their slot elements are described in Table 1.

For an ideal Butler network, the injected signal is divided equally between the output ports with an expected insertion loss of 6 dB at the output terminals. The challenge in the design is to minimize the losses and maintain the required phase difference between the output ports feeding the traveling-wave antenna arrays over a large operating bandwidth. In beam switching operation, one port is excited at a time, giving rise to one out of four beam directions. Other wideband designs have also been implemented and reported in the literature as recently reported in Ref. 13.

The slot antenna element is chosen in this work because of its easy implementation and simple integration within the ground plane. The designed slot antenna, which has a width of 0.4 mm, is fed by the 50-Ω microstrip feeding line. For the 2 × 4 structure, the slot's center is shifted by 1.3 mm from the

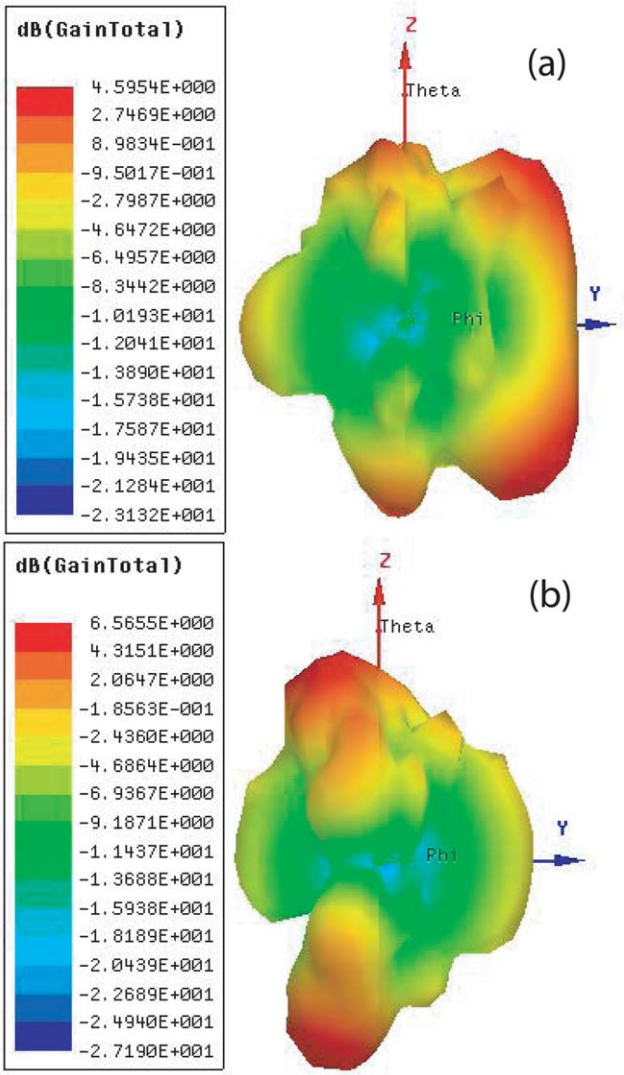

Figure 3 Simulated 3D Gain pattern for the 4 × 4 antenna array integrated with Butler at 28.5 GHz when (a) Port 1 or (b) Port 2 is excited. [Color figure can be viewed in the online issue, which is available at wileyonlinelibrary.com]

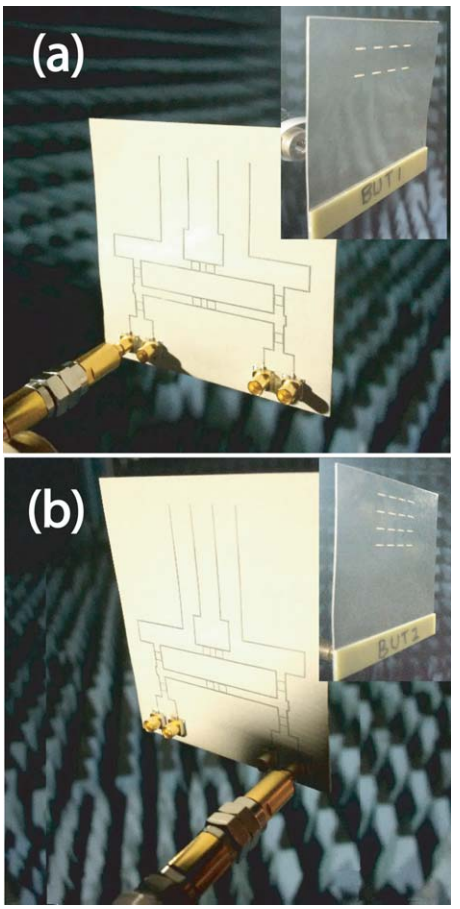

Figure 4 The top view of the fabricated models for the: (a) 2 × 4 and (b) 4 × 4 antenna array. Inset pictures show the back view of the antennas. [Color figure can be viewed in the online issue, which is available at wileyonlinelibrary.com]

center of the feeding line for 50-Ω matching. It has a length of half a wavelength, which has been optimized through simulations to 3.45 mm. The spacing between the centers of the adjacent slots is 6.9 mm. The proposed planar arrays utilize parallel feeding such that each microstrip feeding line excites a series array of slots defining a traveling-wave antenna. As a result, the overall size of the 2 × 4 and 4 × 4 antenna systems are 55.2 × 55 × 0.13 mm^3 and 53.7 × 61.2 × 0.13 mm^3, respectively.

3. RESULTS AND DISCUSSIONS

The optimization and simulations of the design were performed using HFSS™. Also, the phase delay lines within the feeding network were optimized to provide the required insertion phases at the input of the antenna arrays. Due to the use of mini-SMP connectors as external ports in the individual Butler design, as well as inputs in the complete system design, pads were placed around the ports with ground connected vias. The use of mini-SMP connectors also placed another restriction which was that the minimum distance between the input lines had to be greater than 5 mm [14]. This resulted in an increased separation of the input mini-SMP connectors from the Butler matrix feed system

When Port 1 was excited, within the Butler matrix, the simulated power levels detected at the output ports varied from −10.4 to −6.1 dB while they varied from −9.3 to −7.6 dB for port 2. For the phases when Port 1 was excited, the phase differences between the output ports was −51.5° between Ports 5 and 6, −42.5° between Ports 6 and 7, and −48.9° between Ports 7 and 8. That introduces an average error of 4° from the ideal difference of −45°. For the second port, the differences were 144.4°, 133.4°, and 122.74° which make an average phase shift of 7.7° from the ideal values of 135°. Tuning the network to obtain the required phase differences between the output ports was quite challenging. That was due to two main factors. The first one was to monitor the amplitude response and not to introduce more losses, while the second issue was the difficulty of tuning the phase differences between all the array input phases.

Figure 2 shows the simulated reflection coefficient curves for all input ports for the 4 × 4 design as well as its port coupling. A slight shift in the desired resonance frequency is observed (i.e., now it is 29 GHz). Similar values were observed for the 2 × 4 antenna structure. The simulated 3D gain patterns for the complete millimeter-wave, switched beam traveling-wave antenna array are shown in Figure 3. A maximum value of ∼4.6 dB was pointing at $\theta = 45°$ and 135° from the z-axis when Port 1 was excited for the 4 × 4 array. When Port 2 was excited, the beam went to −20° and −160°, with 6.5 dBi gain. Similar behavior was observed for the 2 × 4 design, with slightly lower gain values (4.1 and 6.4 dBi for Ports 1 and 2, respectively). The other two ports behaved similarly.

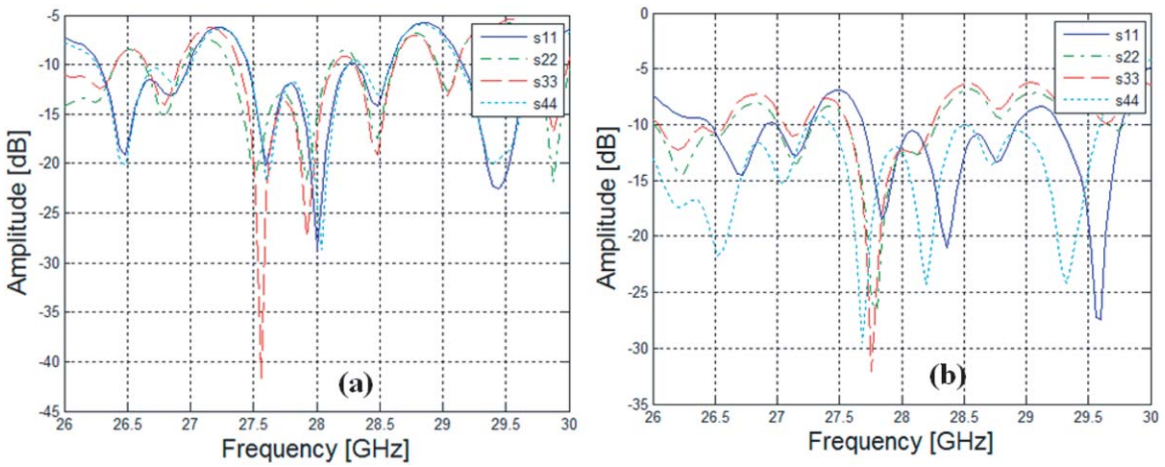

Figure 5 Measured reflection coefficients for (a) the 2 × 4 antenna array system (b) the 4 × 4 antenna array system. [Color figure can be viewed in the online issue, which is available at wileyonlinelibrary.com]

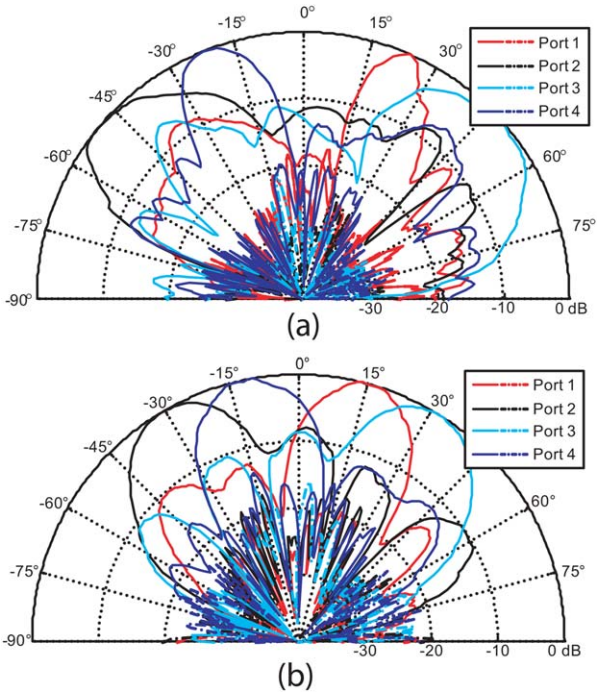

Figure 6 Measured patterns at (a) 27.6 GHz for the 2 × 4 antenna system for all ports, (b) 27.8 GHz for the 4 × 4 antenna system for all ports (continous line co-pol values, dashed-dotted line x-pol levels). [Color figure can be viewed in the online issue, which is available at wileyonlinelibrary.com]

Photographs of the fabricated prototypes are shown in Figure 4 with front and back views. The responses experienced a frequency shift of ∼1 GHz when comparing simulations against measurements due to the fabrication tolerances and possible material variations. In addition, the connector model was not incorporated into the simulations, only its pad. The measured input port *S*-parameters for the two designs are shown in Figure 5 and were conducted at KFUPM, Saudi Arabia, using an Agilent PNA (N5572A). As can be noted from Figure 5(a), Port 1 of the 2 × 4 antenna array system has a BW of 720 MHz centered at 26.64 GHz and 800 MHz from 27.44 to 28.44 GHz. A 1 GHz BW is achieved by Port 2 centered at 25.95 GHz. It also has a BW of 760 MHz centered at 27.7 GHz. It can be summarized that the 2 × 4 antenna array provided a BW of about 0.8 GHz centered around 27.8 GHz for all ports. For the 4 × 4 design, Port 1 achieved a measured BW of 1.24 GHz centered at 28.3 GHz. The second port has 720 MHz centered at 27.9 GHz and 1.04 GHz at 26.1 GHz. The overall BW of the 4 × 4 array is about 0.8 GHz centered at 28 GHz.

The radiation patterns for both designs were measured in the anechoic chamber facility at the Royal Military College of Canada, ON, Canada, and the University of Michigan, Ann Arbor, USA. Figures 6(a) and 6(b) show the normalized measured patterns for the two arrays for their upper halves. The beams were successfully steered from broadside with peak gains ranging from 5 to 7 dBi. The 2 × 4 array had wider beamwidths for Ports 2,3 compared to 1,4, while the 4 × 4 array had comparable beamwidths for all ports due to array symmetry.

4. CONCLUSION

In this work, two versions (2 × 4 and 4 × 4) of millimeter-wave beam switching antenna arrays have been designed, fabricated, and measured. The feeding network was based on a Butler matrix and slot elements were employed within the traveling-wave phased arrays. The overall antenna sizes were 55.2 mm by 55.0 mm by 0.13 mm and 53.7 mm by 61.2 mm by 0.13 mm, nominating them as suitable short-range solutions for handheld devices. The minimum measured BWs were 0.8 GHz and 0.7 GHz for the 2 × 4 and the 4 × 4 antenna structures, respectively, and both cover the 28 GHz band of operation. The peak gain for the antenna systems (feed network and arrays) ranged from 5 to 7 dB.

ACKNOWLEDGMENT

The authors would like to acknowledge the support provided by the Deanship of Graduate Research (DSR) at King Fahd University of Petroleum and Minerals (KFUPM), Dhahran, Saudi Arabia, under project number RG1332.

REFERENCES

1. T.S. Rappaport, S. Sun, R. Mayzus, H. Zhao, Y. Azar, K. Wang, G.N. Wong, J.K. Schulz, M. Samimi, and F. Gutierrez, Millimeter wave mobile communications for 5G cellular: It will work! IEEE Access (2013), 335–349.
2. T. Rappaport, F. Gutierrez, E. Ben-Dor, J. Murdock, Y. Qiao, and J. Tamir, Broadband millimeter-wave propagation measurements and models using adaptive-beam antennas for outdoor urban cellular communications, IEEE Trans Antennas Propag 61 (2013), 1850–1859.
3. P. Baccarelli, P. Burghignoli, C. Di Nallo, F. Frezza, A. Galli, P. Lampariello, and G. Ruggieri, Full-wave analysis of printed leaky-wavephased arrays, Int J RF Microwave Comput Aided Eng 12 (2002), 272–287.
4. M.A.Y. Abdalla and G.V. Eleftheriades, A planar electronically steerable patch array using tunable PRI/NRI phase shifters, IEEE Trans Microwave Theory Tech 57 (2009), 531–541.
5. Y.K. and B. Lee, Beam scannable patch array antenna employing tunable metamaterial phase shifter, In IEEE Antennas and Propagation Society International Symposium (APSURSI), Chicago, IL, 2012.
6. P. Loghmannia, M. Kamyab, M. RanjbarNikkhah, and R. Rezaiesarlak, Miniaturized low-cost phased array antenna using SIW slot elements, IEEE Antennas Wireless Propag Lett 11 (2012), 1434–1437.
7. C.H. Tesng, C.J. Chen, and T.H. Chu, A low-cost 60-GHz switched-beam patch antenna array with Butler matrix network IEEE Antennas Wireless Propag Lett 7 (2008), 432–435.
8. C.E. Patterson, W.T. Khan, G.E. Ponchak, G.S. May, and J. Papapolymerou, A 60-GHz active receiving switched-beam antenna array with integrated Butler matrix and GaAs amplifiers, IEEE Trans Microwave Theory Tech 60 (2012), 3599–3607.
9. S. Gruszczynski and K. Wincza, Broadband 4 × 4 Butler matrices as a connection of symmetrical multisection coupled-line 3-dB directional couplers and phase correction networks, IEEE Trans Microwave Theory Tech 57 (2009), 1–9.
10. C. Liu, S. Xiao, Y.X. Guo, M.C. Tang, Y.Y. Bai, and B.Z. Wang, Circularly polarized beam-steering antenna array with Butler matrix network, IEEE Antennas Wireless Propag Lett 10 (2011), 1278–1281.
11. T.Y. Chin, S.F. Chang, C.C. Chang, and J.C. Wu, A 24-GHz CMOS Butler Matrix MMIC for multi-beam smart antenna systems, In: Radio Frequency Integrated Circuits Symposium, Atlanta, GA, 2008, pp. 633–636.
12. R.L. Haupt, Array beamforming networks, In: Antenna arrays—A computational approach, Hoboken, New Jersey, Wiley, 2010, pp. 408–460.
13. O. Haraz and A.-R. Sebak, Two-layer butterfly-shaped microstrip 4 × 4 Butler matrix for ultra-wideband beam-forming applications, In 2013 IEEE International Conference on Ultra-Wideband (ICUWB), 2013.
14. Pasternack Enterprises, Mini SMP Male Full DetentConnector Solder Attachment Surface Mount PCB, 2014. Available online at: http://www.pasternack.com/images/ProductPDF/PE44489.pdf.] Accessed December 16, 2015.